PVDF/$BaTiO_3$ Composite Foams with High Content of β Phase by Thermally Induced Phase Separation (TIPS)

Aleksandra Bužarovska[a]*, *Mateja Kubin*[a], *Petre Makreski*[b], *Michele Zanoni*[c], *Leonardo Gasperini*[d], *Giacomo Selleri*[d], *Davide Fabiani*[d,e], *Chiara Gualandi*,[c,e]

[a] *Ss. Cyril and Methodius University, Faculty of Technology and Metallurgy, Rudjer Boskovic 16, 1000 Skopje, N. Macedonia*
*E-mail: abuzar@tmf.ukim.edu.mk

[b] *Ss. Cyril and Methodius University in Skopje, Faculty of Natural Sciences and Mathematics, Institute of Chemistry, Arhimedova 5, 1000 Skopje, N. Macedonia*

[c] Department of Chemistry "Giacomo Ciamician" and INSTM UdR of Bologna, University of Bologna, Via Selmi, 2, 40126 Bologna, Italy

[d] *Department of Electrical, Electronic, and Information Engineering, University of Bologna, Viale Risorgimento 2, 40136 Bologna, Italy*

[e] *Interdepartmental Center for Industrial Research on Advanced Applications in Mechanical Engineering and Materials Technology, CIRI-MAM, University of Bologna, Viale Risorgimento, 2, 40136 Bologna, Italy*

Abstract

Poly(vinylidene fluoride) (PVDF) displays ferroelectric, piezoelectric and pyroelectric behavior and it is widely used in high-tech applications including sensors, transducers, energy harvesting devices and actuators. The crystallization of this polymer into highly polar β phase is desirable but is hard to achieve without applying specific thermo-mechanical treatments. Indeed, fabrication processes directly affect PVDF molecular chain conformation, inducing distinct polymorphs. In this paper, we present the fabrication of PVDF/$BaTiO_3$ composite foams by thermally induced phase separation method (TIPS). Different compositions are tested and characterized. The crystallinity, and in particular the development of electroactive β crystal phase is monitored by FTIR, DSC and XRD measurements. Dielectric properties are also evaluated. It turns out that TIPS is a straightforward method that clearly promotes the spontaneous growth of the β phase in PVDF and its composite foams, without the need to apply additional treatments, and also significantly improves the degree of crystallinity. $BaTiO_3$ content gives additional value to the development of β phase and total crystallinity of the systems. The low permittivity values (between 2 and 3), combined with the cellular morphology makes these materials suitable as lightweight components of microelectronic circuits.

Keywords: poly(vinylidene fluoride), thermally induced phase separation (TIPS), foams, crystallinity, β phase, barium titanate, permittivity

Introduction

In the last 15 years, a significant scientific attention has been dedicated to energy harvesting systems based on either piezoelectric or pyroelectric materials, capable of converting mechanical energy and temperature fluctuation into electricity. As typical electroactive polymers, poly(vinylidene fluoride) (PVDF) and its copolymers were widely studied from various aspects [1-3]. PVDF crystallizes in five different crystalline forms (α, β, γ, δ and ε), but only the β crystal phase is piezoactive under certain conditions [4,5]. The relative amount of these crystalline

polymorphs largely depends on the manufacturing process and several approaches have been applied in order to promote the crystallization of the electroactive β phase, such as mechanical stretching, spin-coating, and electrospinning [5,6]. Besides the processing techniques, certain incorporated fillers might also act as nucleators favoring the desired crystal phase in composite systems [7-9]. Inorganic piezoelectric fillers, such as PZT, $BaTiO_3$, ZnO, AlN, are extensively used to enhance the performance of PVDF [10].

A typical example is the PVDF/$BaTiO_3$ organic-inorganic pair. $BaTiO_3$ belongs to perovskite-type ceramics with interesting properties, possessing very high piezo and dielectric constants combined with its eco-friendlier character compared to all other ceramics based on lead [11,12]. A large number of PVDF/$BaTiO_3$ composites were processed by various methods [13-16] obtaining different crystal phases as a result of different applied solvents, polymer solution concentrations and thermal annealing treatments, as well as different solution casting substrates. Typically, applying various methods, α phase was primarily developed with different fractions of β and γ phases. Limited scientific attention was dedicated to PVDF composite foams, aiming to achieve high content of β phase and high degree of crystallinities. Lanceros-Mendez *et al.* have reported the production of electroactive 3D PVDF scaffolds by different approaches, such as NaCl salt leaching, solvent casting, and freeze extraction with nylon and poly(vinyl alcohol) templates. However, the obtained degrees of crystallinities were low, between 33% and 47% [17]. Similar composite foams with excellent piezoelectric properties were produced by sugar-templating strategy, using polydimethylsiloxane as a matrix, and $BaTiO_3$ nanoparticles and carbon nanotubes as nanofillers [18]. Since some works have demonstrated that foaming could enhance the electrical and dielectric properties, highly loaded piezoelectric thermoplastic polyurethane/lead zirconate composite foams were developed using expandable microspheres responsible for creating highly cellular structure [19]. Numerous PVDF foams were produced for various other applications such as insulating materials and materials used in separation processes [20,21]. In these systems, limited attention has been devoted to the crystal structure, the development of certain crystal phase, and the parameters that tune the desired piezoelectric properties.

In the present study, PVDF/$BaTiO_3$ composite foams were produced by thermally induced phase separation method (TIPS). A comprehensive structural analysis was performed in order to study the influence of the fabrication process and the content of $BaTiO_3$ micro-sized filler on the development of highly desirable electroactive β-phase and overall degree of crystallinity. The observed synergy between these two aspects is believed to be crucial in the development of high β-phase content (up to 73.5%) and high degree of crystallinity (up to 87%), giving these composite foams a great potential as piezo-sensing materials. The cellular structure was shown to have a huge impact on the dielectric properties of the produced foams, exhibiting low-k-dielectric characteristics, widely used in microelectronics.

Materials and Methods

Materials

PVDF polymer (Solef 6008) with density of 1.75 g/cm^3 was kindly supplied by Solvay Specialty Polymers (Italy). Dimethyl sulfoxide (DMSO) with 99.5% purity (Merck product) was used as a solvent. Barium titanate (IV) (99%) powder, with particle size between 0.85-1 μm, was a product of Acros Organics. All chemicals were used as received, without previous purification.

Preparation of Composite Foams

Composite foams were produced by thermally induced phase separation method, as a simple and cost-effective approach [22]. The corresponding PVDF/$BaTiO_3$ composite foams were prepared as 5 wt% solutions in DMSO. The polymer solutions were heated up to 40 °C for 24 h, in order to obtain transparent solutions. After that, an appropriate amount of $BaTiO_3$ powder was added to the resulting solutions, mechanically stirred for 1 h, and ultrasonically treated for additional 3 h. The suspensions were then poured into Petri dishes and frozen at -35 °C. The glass dishes side walls were protected with a thick PTFE layer, and the bottom side was positioned on metal support in order to provide directional freezing of the suspensions. The DMSO solvent was extracted from the foams, using deionized water as a non-solvent. The created foams were then dried at room temperature. The composition of PVDF/$BaTiO_3$ composite foams and their abbreviations are given in Table 1.

Foams Characterization

Scanning electron micrographs were taken using a Leica Cambridge Stereoscan 360 Scanning Electron Microscope (SEM), operating at an accelerating voltage of 20 kV. Before observation, the samples were sputtered with gold.

FTIR-ATR spectra were recorded with a Perkin Elmer Spectrum 100 FTIR spectrometer (USA) with 32 scans, in the range of 4000−600 cm^{-1}, with a resolution of 4 cm^{-1}.

Thermogravimetric analyzer (TGA, Q500, TA instruments) was used to determine the thermal stability of the as-prepared composite foams in the temperature range between 30 °C and 700 °C, with a heating rate of 10 °C min^{-1}. All measurements were performed under constant air flow.

Thermal transitions were determined with a TA Instruments differential scanning calorimeter, DSC Q100, equipped with a refrigerated cooling system (RCS). The samples were subjected to a first heating scan at 10 °C min^{-1} from -90 °C to 200 °C, a controlled cooling at 10 °C min^{-1} up to -90 °C, and a second heating scan at 10 °C min^{-1}. The degree of crystallinity X_c was determined using Equation 1:

$$X_c = \frac{\Delta H_m}{\Delta H_m^o \cdot w_{PVDF}} \times 100 \qquad (1)$$

where ΔH_m is melting enthalpy determined in the first heating scan, ΔH_m^o is enthalpy of hypothetically 100% crystallized PVDF, taken as 104.7 J g^{-1}, [23,24] and w_{PVDF} is PVDF weight fraction in the corresponding composite foam.

X-ray Diffraction (XRD) measurements were performed on a Rigaku Ultima IV powder X-ray diffractometer, within 2θ range from 10 to 80°, applying a scanning rate of 0.02 ° min^{-1}. CuK_α radiation was obtained from a generator set at 40 kV and a current of 40 mA. To extract the relevant XRD peaks and their intensities (integrated area), the curve-fitting was performed using Grams AI™ Spectroscopy Software. The crystallinity index (X_c) was determined using Equation 2:

$$X_c = \frac{\sum A_c}{\sum A_c + \sum A_a} x100\% \qquad (2)$$

where $\sum A_c$ and $\sum A_a$ are the total integrated areas of the crystalline peaks and amorphous halo, respectively.

Dielectric Measurements

Dielectric spectroscopy measurements were performed using a Novocontrol Alpha Dielectric Analyzer v2.2. It is based on a high voltage amplifier for the application of a variable frequency electric field on the sample. The measuring cell consists of a lower electrode for the application of high voltage, and a grounded upper electrode for signal acquisition.

The instrument measures the material impedance, capacitance (C) and dielectric loss (tanδ). The dielectric properties of the material (i.e. the real and imaginary parts of permittivity) are indirectly calculated once noted the geometric dimensions of the sample (thickness and diameter). The dielectric constant of the material ε_r is then calculated by using Equation 3:

$$\varepsilon_r = \frac{C}{\varepsilon_0} \cdot \frac{d}{S} \qquad (3)$$

where ε_0 is the permittivity in vacuum (8.85×10^{-12} F m^{-1}), S is the thickness of the sample, and d is the diameter of the high voltage electrode of the cell. The equipment was set by applying 500 V_{rms} over a frequency range from 10^{-1} to 10^{4} Hz.

Results and Discussion

Morphology Observation

PVDF-BT composite foams with different amounts of $BaTiO_3$ were produced by TIPS as flexible thin discs of approximately 4 cm in diameter and about 500 µm thick (**Figure 1**).

The SEM images reported in **Figure 2** provide information about the 3D microstructure, pore dimensions, and the quality of particle dispersion. The foams displayed a highly porous interconnected structure with pores having dimensions in the range of 10-40 µm, with pure PVDF displaying bigger pores with respect to the composites. The reduction of pore dimension in the composites might be attributed to heterogeneous nucleation and increased number of nucleation sites upon the addition of $BaTiO_3$ particles [25]. High-magnification images of the composites show the presence of $BaTiO_3$ particles, having a diameter of few microns, as expected. The amount of $BaTiO_3$ particles, detectable on the surface of the pore walls, increased with the increase of the ceramic loading, thus supporting the nominal amount of $BaTiO_3$ added during the foam preparation. It is worth mentioning that when $BaTiO_3$ concentration exceeded 10 wt%, some of the particles where not completely embedded in the polymer matrix, as detectable in Figure 2h and j.

FTIR Spectroscopy Characterization of β-Phase Content

The FTIR spectra of the PVDF and PVDF composite foams were recorded to determine the relative fraction of the developed β phase. **Figure 3** shows normalized FTIR spectra of all as-prepared foams. Special attention was given to the assignation of crystalline sensitive peaks. The absorption bands positioned at 762 cm^{-1} [ρ(CF-CH-CF)], 795 cm^{-1} [ρ(CF_2)] and 975 cm^{-1} [δ(CH_2)] were attributed to the presence of α phase [5,26], while the bands located at 872 cm^{-1} [(δCH_2)] and 838 cm^{-1} [ρ(CH_2)] were attributed to the presence of β phase [5,26]. Deformation vibration bands of CH_2 groups, positioned at 1453 cm^{-1} and 1402 cm^{-1} were also relevant to the presence of β phase [26]. Similar absorption bands were detected in all composite foams with no obvious absorption band shifting, suggesting an absence of specific interaction between PVDF matrix and $BaTiO_3$ filler, as expected.

The relative fraction of the β phase was determined according to Equation 4:

$$F(\beta) = \frac{A_\beta}{\left(\frac{K_\beta}{K_\alpha}\right)A_\alpha + A_\beta} = \frac{A_\beta}{1.26A_\alpha + A_\beta} \times 100 \qquad (4)$$

where the absorption coefficients, K_α is 6.1x10^4 and K_β is 7.7x10^4 cm^2 mol^{-1}, while A_α and A_β are absorbances at 762 cm^{-1} and 838 cm^{-1}, respectively [27]. The *F(β)* for the PVDF powder was only 27%, while after the foaming process PVDF displayed a higher β phase content of 64%. The addition of 10 and 20 wt% of $BaTiO_3$ further increased the β phase content to 72.1% and 73.8% for PVDF-10BT and PVDF-20BT, respectively, suggesting that the incorporation of $BaTiO_3$ improved the development of electroactive β phase. The lower *F(β)* values in PVDF-5BT and PVDF-15BT (55.8% and 60.9%, respectively), might be due to the fact that the widely used FTIR approach for determination of *F(β)* usually does not take into consideration the absorption peaks in the wavenumber range of 400-1500 cm^{-1}, exclusively relevant to the β and γ phases [26]. However, compared to literature data, even unfilled PVDF foam exhibited significant fraction of β phase, probably as a result of applied temperature gradient during the foams preparation. The polar nature of the used DMSO solvent might have additional influence in favoring the formation of the β phase [27].

Thermal Properties

The TGA curves and the corresponding derivatives are presented in Figure 4a and b. All TGA curves had a similar trend in the investigated temperature region. The onset temperatures and the corresponding weight residues are given in Table 2. In air, PVDF degraded in two distinct mass loss steps with no residual weight, as previously reported [28]. Conversely, $BaTiO_3$ was stable within the same temperature range. In the composites, the residual weight after the complete decomposition of the polymeric components corresponds to $BaTiO_3$ content; values are reported in Table 2 and are perfectly in line with the nominal composition, within the accuracy of TGA quantification. Notably, the main DTG peak in PVDF was located at 470 °C, denoting the temperature at maximum rate of mass loss, while in PVDF/$BaTiO_3$ foams this main peak was shifted to significantly lower values with the increase of $BaTiO_3$ content. It is interesting to note that in composite foams, a new DTG peak was detected at around 400 °C, with a tendency to shift to higher temperatures with the increase of filler content. Therefore, our results show a decrease of PVDF thermal stability in presence of $BaTiO_3$, whereas previous studies reported an opposite effect of $BaTiO_3$ on polymer thermal degradation [29,30]. This discrepancy can be ascribed to the different atmospheres under which thermal stability was evaluated, i.e. air in the present study, and inert gas in the cited literature [14].

DSC thermograms (I heating run) of PVDF/$BaTiO_3$ composite foams, in a temperature region between -90 °C and 200 °C are shown in Figure 4c, and corresponding calorimetric data are reported in Table 3. In the first heating scan, the absence of a detectable stepwise specific heat increment, ascribable to the glass transition, and the presence of two melting endotherms clearly show that the polymer is highly crystalline. The low-T endotherm is centered at 68 °C, while the second melting peak occurs in the expected temperature region (around 170 °C). In literature, the endotherm peak at lower temperatures, which disappears in the second heating scan, is typical of PVDF annealed at room temperature and is usually ascribed to unstable secondary crystals [31,32]. Other origins have been also reported, such as upper glass transition [33], melting of paracrystalline domains [34], or α-relaxation in the crystalline/amorphous interface [23].

It is sometimes difficult to distinguish the regular melting peaks of different types of crystal phases in PVDF (α, β or γ), since they differ from each other by only a few degrees [35]. According to the reference data, the melting

peak of PVDF in the range of 165-172 °C usually corresponds to the melting of β crystal phase, while the range of 172-175 °C is generally associated with the melting of α crystal phase. From this point of view, it could be concluded that the melting peaks (mostly around 169 °C in all investigated samples) reflected the presence of the β phase, induced in higher fraction than α crystal phase. The degree of crystallinity was estimated based on a sum of the melting enthalpies corresponding to the lower and upper melting peaks. The degree of crystallinity of pure PVDF foam was 79.5%, while for PVDF composite foams it had higher values (between 82.1% and 87.0%) (Table 3). The composites containing 10 and 15 wt% of $BaTiO_3$ displayed the highest crystallinity degree, thus confirming previous data reporting the effect of $BaTiO_3$ in promoting PVDF crystallization [36]. Taking into account these high degrees of crystallinity and the high values of relative β phase fraction, determined by FTIR spectroscopy, these systems could be identified as potential piezoelectric materials.

During the second heating scans (Figure 4d, Table 3), it could be recognized that the lower melting peak (around 68 °C, detected in the first heating scan) is absent, with a clearly defined single melting peak around 171 (±1) °C. The slight shift of the melting peaks in the upper temperature region to higher values (between 170-172°C), observable for all investigated foams, could be a result of diminishing the presence of β phase during the crystallization process from polymer melt, leading to the development of less desired α phase [37]. The degrees of crystallinity (II run), collected in Table 3, were also lower (70.7%-73.5%) than those derived from the first heating runs, thus supporting the fact that the preparation procedure gives additional value to the overall degree of crystallinity and promotes the formation of the β phase. Despite the fact that the crystallinity is lower when compared to X_c's from the first runs, it is significantly higher when compared to other PVDF/$BaTiO_3$ composites, which are already published in literature [33].

Microstructural Analysis

In order to identify and distinguish the presence of different crystalline phases, the XRD analysis was performed. Although it was quite challenging, this important step is of vital importance to determine the developed crystalline phases in PVDF polymer. The collected XRD patterns of PVDF, its composite foams and $BaTiO_3$ (inset) are presented in Figure 5a.

Three main maxima at 18.4°, 19.9° and 26.4° (2θ) were registered in the pure PVDF foam, corresponding to (020), (110) and (021) reflections of the monoclinic α phase [5,26,38,39]. In addition, the two less intensive peaks observed at 36° (200) and 39° (132) are characteristic peaks for α and γ crystal phases, respectively [38,40]. As expected, all diffraction peaks attributed to PVDF phase decreased their intensity with the increase of $BaTiO_3$ content.

Another important aspect, observed from the XRD patterns (Figure 5b) of the composite foams, is the consistent upshift of the mean peak (from 19.9° towards 20.1° by increasing $BaTiO_3$ content). Additionally, the peak located at 26.4° in the bare PVDF foam decreased its intensity in the PVDF composite foams with the increase of $BaTiO_3$ content (Figure 5a and 5b), suggesting diminishing presence of the α crystal phase.

The presence of the orthorhombic β crystal phase is usually associated to the appearance of the 2θ peak between 20.3° and 20.8°, which is obviously not visualized as a separate peak. However, the accurate deconvolution of the wide broad peak, centered at 20.1°, revealed the presence of the peak at 20.6°, and the β crystal phase was determined in pure PVDF foam and in all composite foams (Figure 5c). The results, pointing to the quantitative presence of the crystalline forms, and the degree of crystallinity of the samples, are summarized in Table 4.

Relatively high contents of β phase (between 54.4 and 68.5 %) were detected in the composite foams and the unfilled PVDF foam. The results correspond nicely with those derived from the FTIR spectroscopy.

The degree of crystallinity, calculated as a ratio of the sum of integrated areas of all peaks arising from the crystalline phases, over the total integrated peaks area, varied between 62.5% to 84.6%. The obtained results are in good agreement with the degrees of crystallinity, determined by DSC analysis. Additionally, taking into account the degree of crystallinity solely to PVDF, the determined content of β phase (between 39.9% and 54.6 %) is still high, showing highly developed β phase when compared to literature data for various PVDF/$BaTiO_3$ systems. Following the above mentioned results, the highly developed β phase is primarily a result of the preparation procedure, and is less affected by the different contents of $BaTiO_3$ in its micron size.

Dielectric Properties

The importance of evaluating the dielectric properties arises from the fact that the piezoelectric voltage coefficient (g_{33}) depends on the relative permittivity and Young's modulus of the material as a measure of its stiffness [41]. The dielectric permittivity in PE polymer foams is usually low, but the mechanical flexibility is enhanced as a result of the cellular structure [19].

The real part of the relative permittivity of the samples for a frequency range between 10^{-1} and 10^4 Hz are presented in Figure 6a. No consistent variations of the permittivity were registered by varying the amount of $BaTiO_3$ of the samples. Indeed, the typical relative permittivity of PVDF is in the range 7-10 (for frequencies below 100 Hz), while in case of foams it is significantly lower, i.e. about 2-3 [2]. These low values can be attributed to the dominance of low permittivity air phase in composite foams. The slight differences of the permittivity values among the samples can be ascribed to the different pore size in the composite foams, which was confirmed by the SEM images. Regarding the imaginary part of the permittivity (Figure 6b), similar trends were registered for all samples, with no significant variations measured with respect to the neat PVDF sample.

Conclusion

PVDF composite foams with different content of micro-sized $BaTiO_3$ filler were prepared by thermally induced phase separation method (TIPS), using DMSO as a polar solvent. Foams with highly porous interconnected structures, with pore sizes between 10 and 40 μm, were produced. A detailed structural analysis suggested that this simple and cost-effective technique, together with the presence of $BaTiO_3$ content, has a significant role in the development of β phase content (up to 73.5 %) and high degree of crystallinity (up to 87 %). This result has important implications for the development of lightweight and flexible electroactive components, since the TIPS method provides an opportunity to produce low density structures with an easy access to PVDF electroactive phase. Moreover, low dielectric permittivity values (between 2 and 3 for all investigated foams) might open a new direction in creating low-*k* materials, widely applicable in microelectronics.

Acknowledgements

This work was financially supported by NATO grant -Project number NATO SPS G5772.

Declarations

Conflict of interest The authors declare no conflict of interest.

References

[1] Guo S, Duan X, Xie M, Aw K.C, Xue Q (2020) Composites, fabrication and application of polyvinylidene fluoride for flexible electromechanical devices: A review. Micromachines 11:1076

[2] Xia W, Zhang Z (2018) PVDF-based dielectric polymers and their applications in electronic materials. IET Nanodielectrics 1:17-31

[3] Soulestina T, Ladmiral V, Dos Santos F.D, Améduri B (2017) Vinylidene fluoride- and trifluoroethylene-containing fluorinated electroactive copolymers. How does chemistry impact properties?. Prog Polym Sci 72:16-60

[4] Ruan L, Yao X, Chang Y, Zhou L, Qin G, Zhang X (2018) Properties and applications of the β Phase poly(vinylidene fluoride). Polymers 10:228

[5] Martins P, Lopes A.C, Lanceros-Mendez S (2014) Electroactive phases of poly(vinylidene fluoride): Determination, processing and applications. Prog Polym Sci 39:683-706

[6] Gebrekrstos A, Madras G, Bose S (2019) Journey to electroactive β-polymorph of poly(vinylidenefluoride) from crystal growth to design and applications. Cryst Growth Des 19:5441-5456

[7] Hou Y, Deng Y, Wang Y, Gao H (2015) Uniform distribution of low content $BaTiO_3$ nanoparticles in poly(vinylidene fluoride) nanocomposite: toward high dielectric breakdown strength and energy storage density. RSC Adv 5:72090-72098

[8] Ke K, Pötschke P, Jehnichen D, Fischer D, Voit B (2014) Achieving β-phase poly(vinylidene fluoride) from melt cooling: Effect of surface functionalized carbon nanotubes. Polymer 55:611-619

[9] Sebastian M.S, Larrea A, Goncalves R, Alejo T, Vilas J.L, Sebastian V, Martins P, Lanceros-Mendez S (2016) Understanding nucleation of the electroactive β-phase of poly(vinylidene fluoride) by nanostructures. RSC Adv 6:113007-113015

[10] Mishra S, Unnikrishnan L, Nayak S.K, Mohanty S (2019) Advances in piezoelectric polymer composites for energy harvesting applications: A systematic review. Macromol Mater Eng 304:1800463

[11] Acosta M, Novak N, Rojas V, Patel S, Vaish R, Koruza J, Rossetti G.A, Rödel J (2017) BaTiO3-based piezoelectrics: Fundamentals, current status and perspectives. Appl Phys Rev 4:041305

[12] Gao J, Xue D, Liu W, Zhou C, Ren X (2017) Recent progress on $BaTiO_3$-based piezoelectric ceramics for actuator applications. Actuators 6:24

[13] Li R, Zhao Z, Chen Z, Pei J (2017) Novel $BaTiO_3$/PVDF composites with enhanced electrical properties modified by calcined $BaTiO_3$ ceramic powders. Mater Express 7:536-540

[14] Mendes S.F, Costa C.M, Caparros C, Sencadas V, Lanceros-Méndez S (2012) Effect of filler size and concentration on the structure and properties of poly(vinylidenefluoride)/$BaTiO_3$ nanocomposites. J Mater Sci 47:1378-1388

[15] Mallick S, Ahmad Z, Qadir K.W, Rehman A, Shakoor R.A, Touati F, Al-Muhtaseb S.A (2020) Effect of $BaTiO_3$ on the sensing properties of PVDF composite-based capacitive humidity sensors. Ceram Int 46:2949-2953

[16] Jiang J, Tu S, Fu R, Li J, Hu F, Yan B, Gu Y, Chen S (2020) Flexible piezoelectric pressure tactile sensor based on electrospun $BaTiO_3$/Poly(vinylidene fluoride) nanocomposite membrane. ACS Appl. Mater. Interfaces 12:33989-33998

[17] Correia D.M, Ribeiro C, Sencadas V, Vikingsson L, Oliver Gasch M, Gómez Ribelles J.L, Botelho G, Lanceros-Méndez S (2016) Strategies for the development of three dimensional scaffolds from piezoelectric poly(vinylidene fluoride). Mater Des 92:674-681

[18] McCall W.R, Kim K, Heath C, La Pierre G, Sirbuly D.J (2014) Piezoelectric nanoparticle−polymer composite foams. ACS Appl Mater Interfaces 6:19504-19509
[19] Petrossian G, Hohimer C.J, Ameli A (2019) Highly-loaded thermoplastic polyurethane/lead zirconate titanate composite foams with low permittivity fabricated using expandable microspheres. Polymers 11:280
[20] Zhao B, Zhao C, Wang C, Park C.B (2018) Poly(vinylidene fluoride) foams: a promising low-: K dielectric and heat-insulating material. J Mater Chem C 6:3065-3073
[21] Bentini R, Annalisa P, Rizzi L.G, Athanassiou A, Fragouli D (2019) A highly porous solvent free PVDF/Expanded graphite foam for oil/water separation. J Chem Eng 372:1174-1182
[22] Bužarovska A, Gualandi C, Parrilli A, Scandola M (2015) Effect of TiO_2 nanoparticle loading on Poly(l-lactic acid) porous scaffolds fabricated by TIPS. Composites Part B 81:189-195
[23] Teyssedre G, Bernes A, Lacabanne C (1993) Influence of the crystalline phase on the molecular mobility of PVDF. J Polym Sci B Polym Phys 31:2027-2034
[24] Nakagawa K, Ishida Y (1973) Dielectric relaxation and molecular motions in polyvinylidene fluoride with crystal form II. J Polym Sci Polym Phys Ed 11:1503-1533
[25] Mohammadi M.S, Rezabeigi E, Bertram J, Marelli B, Gendron R, Nazhat S.N, Bureau M.N (2020) Poly(d,l-Lactic acid) composite foams containing phosphate glass particles produced via solid-state foaming using CO_2 for bone tissue engineering applications. Polymers 12:231
[26] Cai X, Lei T, Sun D, Lin L (2017) A critical analysis of the α, β, and γ phases in poly(vinylidene fluoride) using FTIR. RSC Adv 7:15382-15389
[27] Gregori R, Cestari Jr.M (1994) Effect of crystallization temperature on the crystalline phase content and morphology of poly(vinylidene fluoride). J Polym Sci B 32:859-870
[28] Nguyen T (1985) Degradation of poly(vinyl fluoride) and poly(vinylidene fluoride). J Macromol Sci C 25:227-275
[29] Sharma M, Quamara J.K, Gaur A (2018) Behaviour of multiphase PVDF in (1−x)PVDF/(x)$BaTiO_3$ nanocomposite films: structural, optical, dielectric and ferroelectric properties. J Mater Sci Mater Electron 29:10875-10884
[30] Bi X, Yang L, Wang Z, Zhan Y, Wang S, Zhang C, Li Y, Miao Y, Zha J (2021) Construction of a three-dimensional $BaTiO_3$ network for enhanced permittivity and energy storage of PVDF composites. Materials 14:3585
[31] Neidhöfer M, Beaume F, Ibos L, Bernès A, Lacabanne C (2004) Structural evolution of PVDF during storage or annealing. Polymer 45:1679-1688
[32] Montanari U, Cocchi D, Brugo T.M, Pollicino A, Taresco V, Romero Fernandez M, Moore J.C, Sagnelli D, Paradisi F, Zucchelli A, Howdle S.M, Gualandi C (2021) Functionalisable epoxy-rich electrospun fibres based on renewable terpene for multi-purpose applications. Polymers 13:1804
[33] Leonard C, Halary J.L, Monnerie L, Micheron F (1984) DSC studies on the transitions in poly(vinylidenefuoride) and some related copolymers. Polym Bull 11:195-202
[34] Nabata Y (1990) Molecular motion in form-II poly/vinylidene fluoride. Jpn. J. Appl. Phys. 29:2782-2788
[35] Satapathy S, Pawar S, Gupta P.K, Varma K.B.R (2011) Effect of annealing on phase transition in poly(vinylidene fluoride) films prepared using polar solvent. Bull Mater Sci 34:727-733
[36] Gong X, Chen Y, Tang C.Y, Law W.C, Chen L, Wu C, Hu T, Tsui G.C.P (2018) Crystallinity and morphology of barium titanate filled poly(vinylidene fluoride) nanocomposites. J Appl Polym Sci 135:46877

[37] Constantino C.J.L, Job A.E, Simoes R.D, Giacometti J.A, Zucolotto V, Oliveira O.N, Gozzi Jr.G, Chinaglia D.L (2005) Phase transition in poly(vinylidene fluoride) investigated with micro-Raman spectroscopy. Appl Spectrosc 59:275-279

[38] Hasegawa R, Takahashi Y, Chatani Y, Tadokoro H (1972) Crystal structures of three crystalline forms of poly(vynilidene fluoride). Polym J 3:600-610

[39] Gregorio R (2006) Determination of the α, β, and γ crystalline phases of poly(vinylidene fluoride) films prepared at different conditions. J Appl Polym Sci 100:3272-3279

[40] Lei T, Cai X, Wang X, Yu L, Hu X, Zheng G, Lv L, Wang L, Wu D, Sun D, Lin L (2013) Spectroscopic evidence for a high fraction of ferroelectric phase induced in electrospun polyvinylidene fluoride fibers. RSC Adv 3:24952

[41] Petroff C.A, Bina T.F, Hutchison G.R (2019) Highly tunable molecularly doped flexible poly(dimethylsiloxane) foam piezoelectric energy harvesters. ACS Appl Energy Mater 2:6484-6489

List of figures

Abstract

Poly(vinylidene fluoride) (PVDF) displays ferroelectric, piezoelectric and pyroelectric behavior and it is widely used in high-tech applications including sensors, transducers, energy harvesting devices and actuators. The crystallization of this polymer into highly polar β phase is desirable but is hard to achieve without applying specific thermo-mechanical treatments. Indeed, fabrication processes directly affect PVDF molecular chain conformation, inducing distinct polymorphs. In this paper, we present the fabrication of PVDF/$BaTiO_3$ composite foams by thermally induced phase separation method (TIPS). Different compositions are tested and characterized. The crystallinity, and in particular the development of electroactive β crystal phase is monitored by FTIR, DSC and XRD measurements. Dielectric properties are also evaluated. It turns out that TIPS is a straightforward method that clearly promotes the spontaneous growth of the β phase in PVDF and its composite foams, without the need to apply additional treatments, and also significantly improves the degree of crystallinity. $BaTiO_3$ content gives additional value to the development of β phase and total crystallinity of the systems. The low permittivity values (between 2 and 3), combined with the cellular morphology makes these materials suitable as lightweight components of microelectronic circuits.

Colour Figure

Click here to download Colour Figure Fig 1.tif

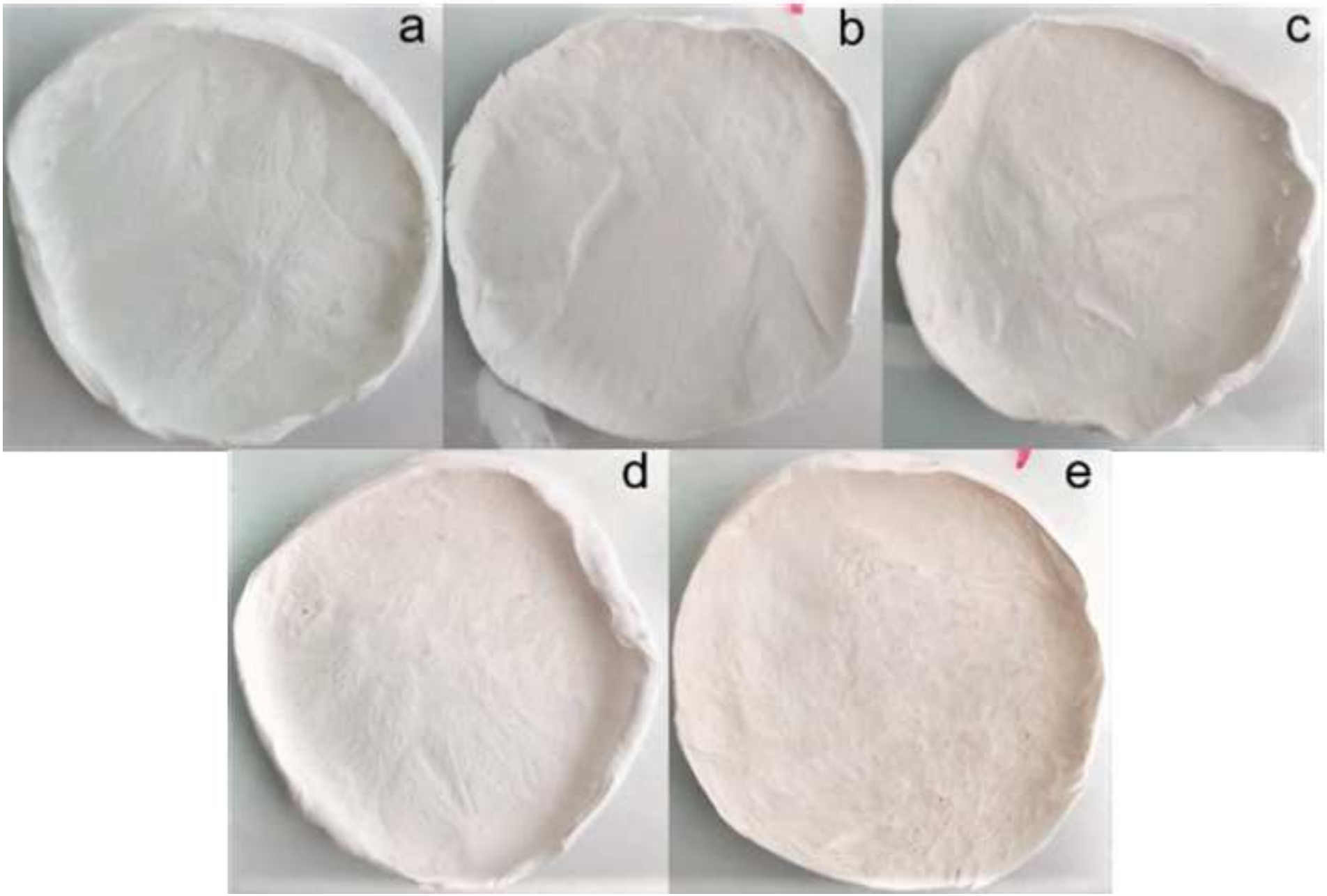

Colour Figure

Click here to download Colour Figure Fig 2.tif

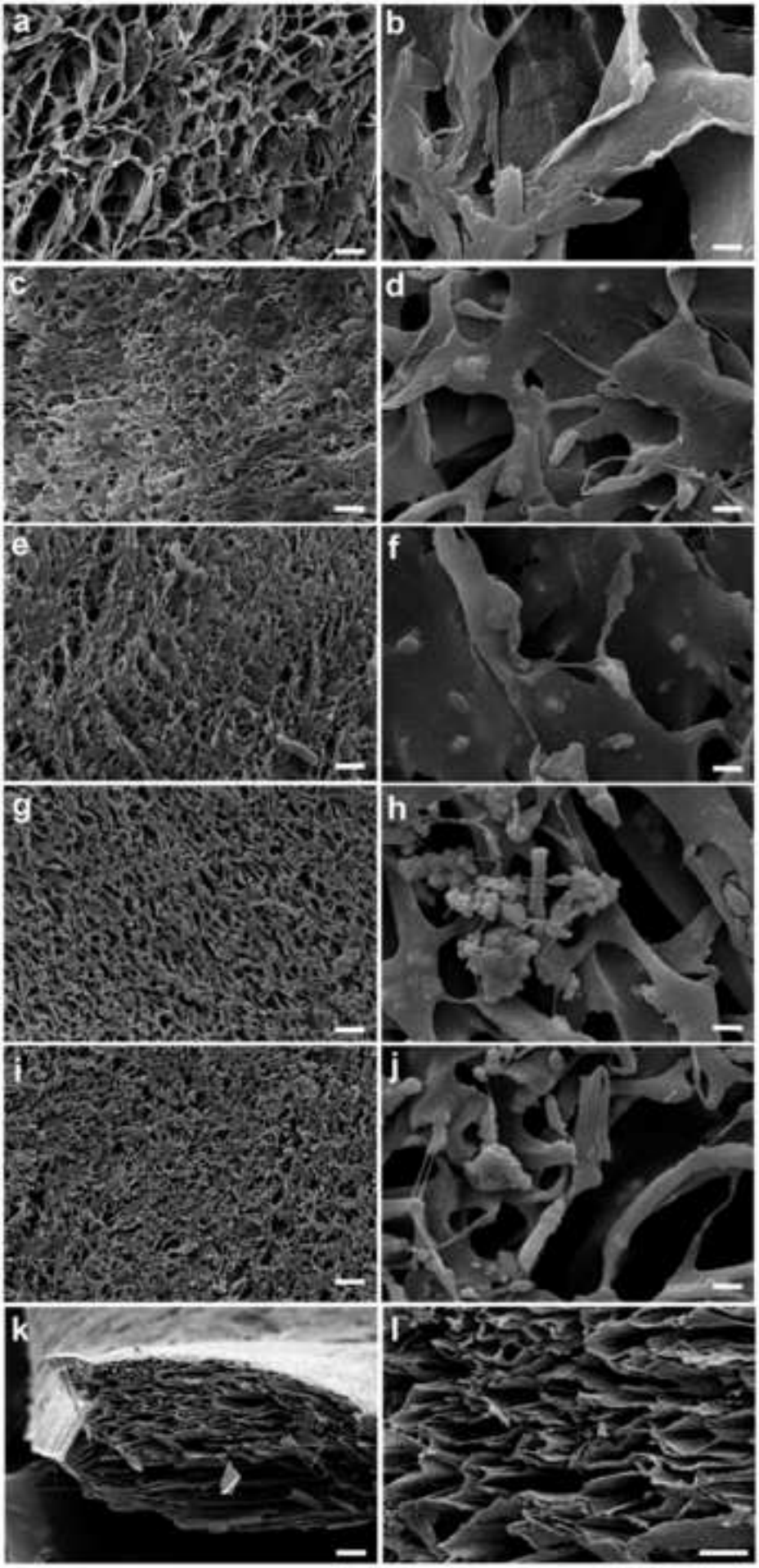

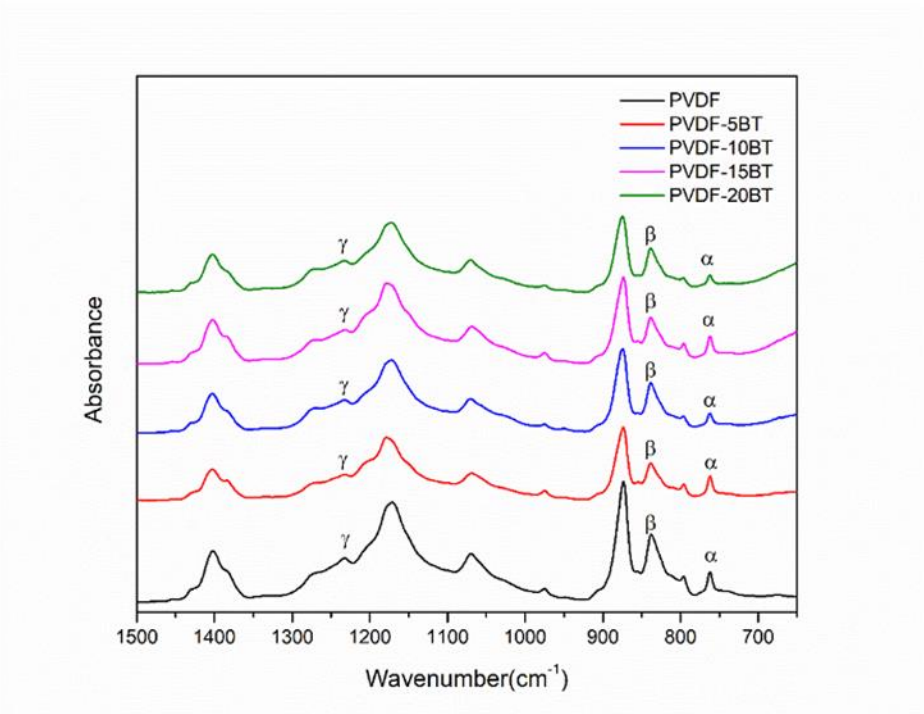

Fig.3

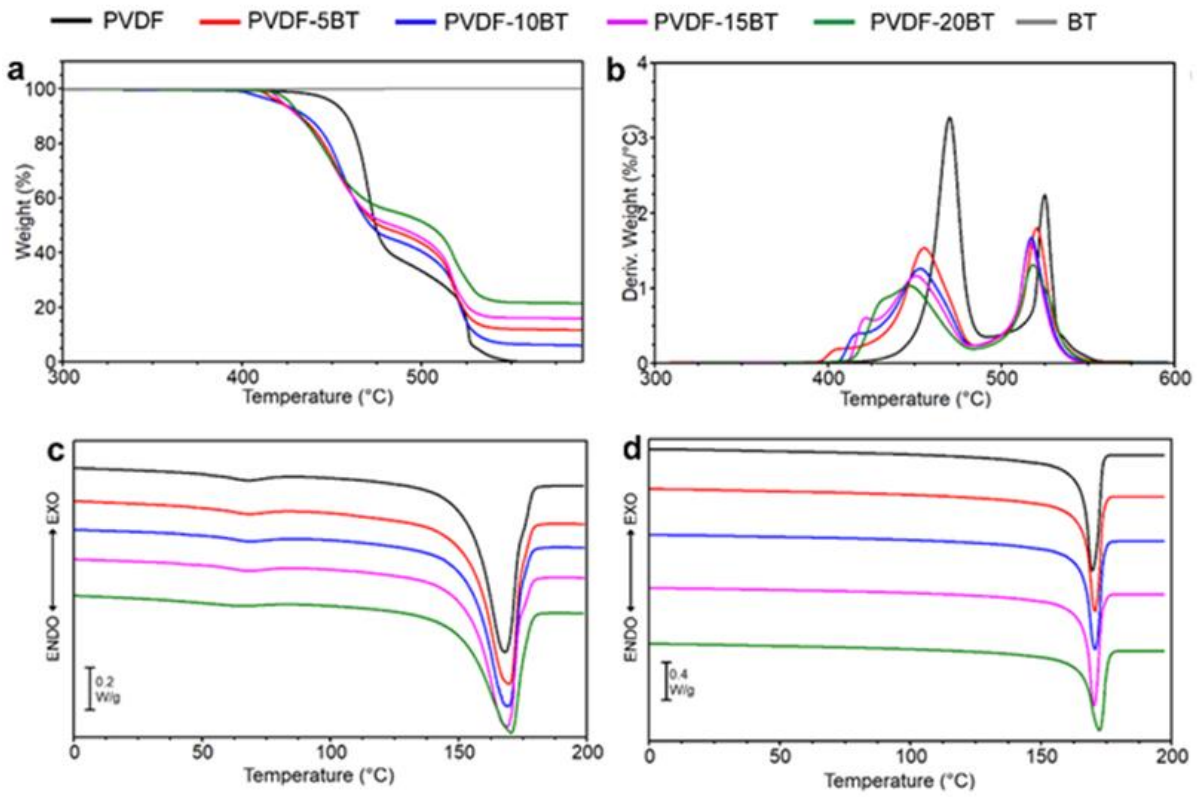
PVDF
PVDF-5BT
PVDF-10BT
PVDF-15BT
PVDF-20BT
BT
a
Weight (%)
Temperature (°C)
b
Deriv. Weight (%/°C)
Temperature (°C)
c
EXO
ENDO
0.2 W/g
Temperature (°C)
d
EXO
ENDO
0.4 W/g
Temperature (°C)

Fig. 4

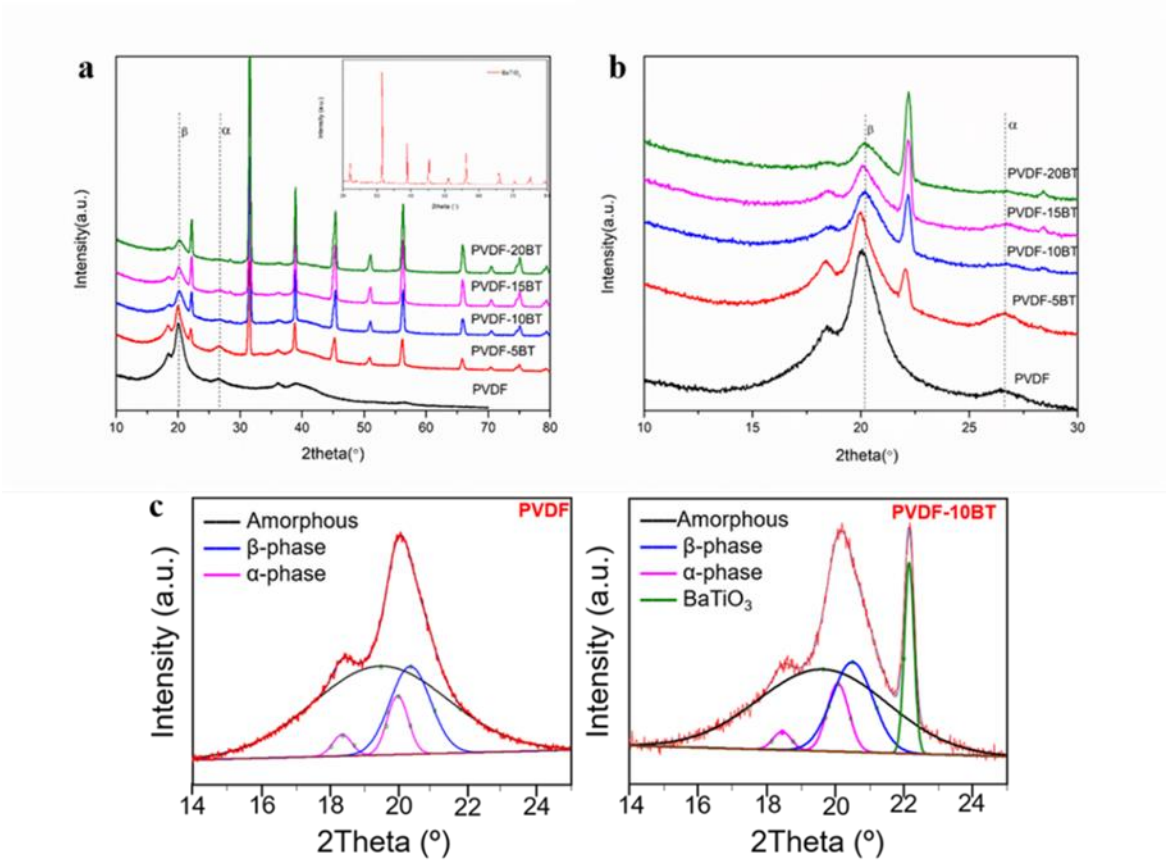
a
Intensity(a.u.)
2theta(°)
PVDF-20BT
PVDF-15BT
PVDF-10BT
PVDF-5BT
PVDF
b
Intensity(a.u.)
2theta(°)
PVDF-20BT
PVDF-15BT
PVDF-10BT
PVDF-5BT
PVDF
c
Amorphous
β-phase
α-phase
PVDF
Intensity (a.u.)
2Theta (°)
Amorphous
β-phase
α-phase
BaTiO3
PVDF-10BT
Intensity (a.u.)
2Theta (°)

Fig. 5

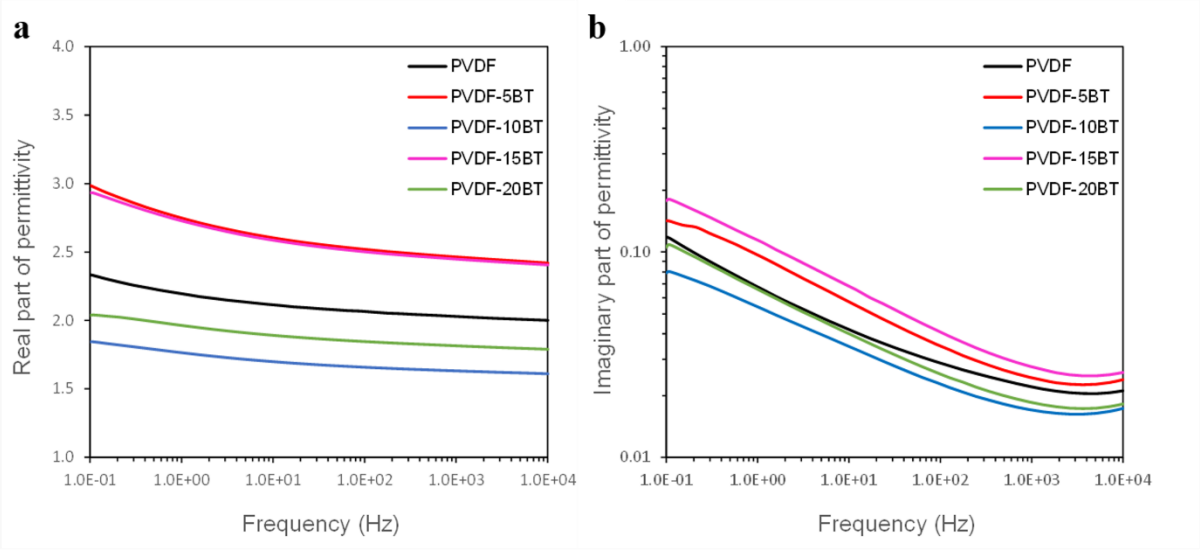

Fig. 6

Table 1. Samples abbreviations and composition of PVDF/$BaTiO_3$ composite foams

Sample code	PVDF/$BaTiO_3$ wt/wt (%)
PVDF	100/0
PVDF-5BT	95/5
PVDF-10BT	90/10
PVDF-15BT	85/15
PVDF-20BT	80/20

Table 2. TGA data of PVDF foam, $BaTiO_3$ (BT) and its composites

Sample	T_{onset} [°C]	T_{deg} [a)] [°C]	m_{res} [b)] %
PVDF	453	470	0
PVDF-5BT	401	455	5.9
PVDF-10BT	412	453	11.6
PVDF-15BT	416	450	15.8
PVDF-20BT	422	447	21.4
BT	n.d.	n.d.	100

[a)]determined by DTG; [b)] at 600°C

Table 3. Calorimetric data of PVDF/$BaTiO_3$ composite foams

	I heating scan					II heating scam		
Sample	$T_{m,1}$ [°C]	$\Delta H_{m,1}$ [J g^{-1}]	$T_{m,2}$ [°C]	$\Delta H_{m,2}$ [J g^{-1}]	X_c [a)] [%]	T_m [°C]	ΔH_m [J g^{-1}]	X_c [b)] [%]
PVDF	68	3.4	168	79.9	79.5	170	74.7	71.3
PVDF-5BT	68	2.8	170	79.6	82.8	171	70.9	71.3
PVDF-10BT	68	3.6	169	78.4	87.0	171	69.3	73.5
PVDF-15BT	68	3.2	169	73.9	86.6	170	64.6	72.6
PVDF-20BT	65	3.1	170	65.7	82.1	172	59.2	70.7

[a)] Calculated by applying Equation 1, where $\Delta Hm = \Delta Hm,_1 + \Delta Hm,_2$
[b)] Calculated by applying Equation 1

Table 4. XRD analysis data of PVDF composite foams

Sample	X_c [%]	$X_{c,PVDF}$[a)] [%]	$X_{c,\beta}$[b)] [%]	X_β[c)] [%]
BT	85.8			
PVDF	62.5		68.5	42.8
PVDF-5BT	74.1	73.5	54.4	39.9
PVDF-10BT	78.9	78.1	67.0	52.3
PVDF-15BT	80.2	79.2	57.6	45.6
PVDF-20BT	84.6	84.4	64.7	54.6

[a)]Estimated degree of crystallinity of PVDF in the composite derived from equation: $\chi_c = \chi_{c,PVDF} \times w_{PVDF} + \chi_{c,BaTiO_3} \times w_{BaTiO_3}$; [b)] Fraction of the β crystal phase over the total crystal phase, calculated as: $\chi_{c,\beta} = \frac{A(\beta)}{A(\alpha+\beta+\gamma)} \cdot 100$, where $A(\beta)$ denotes the area corresponding to the peak of β and $A(\alpha+\beta+\gamma)$ total area of peaks of α, β and γ phases; [c)] Fraction of the β crystal phase, related to $X_{c,PVDF}$